Journal of Geomine (2026), 4(1), 1-16
DOI: 10.22077/jgm.2026.11170.1074

Rock mass sensitivity and stability of unsupported sublevel stopes: An integrated laboratory and numerical study at the Tajkuh lead–zinc mine

Majid Noorian-Bidgoli[1]*, Hossein Jafari[2]

Received: 2026 Apr. 22, Revised: 2026 May 28, Accepted: 2026 Jul. 11, Published: 2026 Jul. 26

ABSTRACT

Ground control and stability assessment of underground excavations are among the most critical aspects of underground mining operations. Instability of underground openings not only compromises safety due to potential rock failure and collapse, but also leads to increased operational costs caused by dilution, production delays, equipment damage, and additional waste handling. This issue becomes particularly significant in unsupported (self-supporting) mining methods such as sublevel stoping, where the stability of excavations relies solely on the inherent strength of the surrounding rock mass. In this study, the stability of underground openings in the Tajkuh lead–zinc mine was investigated using numerical modeling. The mine is currently operated at multiple levels with unsupported stopes. Initially, intact cylindrical core specimens were collected from exploratory drilling and subjected to uniaxial and triaxial compressive tests to determine key geomechanical properties, including cohesion, internal friction angle, density, and elastic parameters. Subsequently, numerical simulations were carried out using FLAC2D finite difference software to evaluate the stability of tunnels with different cross-sectional dimensions (2.5×2.5, 3.5×3.5, and 4.5×4.5 m^2) at varying depths (30, 55, and 80 m). The results indicate that maximum displacement occurs in tunnels with a cross-section of 4.5×4.5 m^2 at a depth of 80 m, whereas minimum displacement is observed for tunnels with dimensions of 2.5×2.5 m^2 at a depth of 30 m. Comparison of the maximum roof displacement with the allowable limits based on the Sakurai criterion demonstrates that all investigated openings remain stable without requiring support systems. Sensitivity analysis further reveals that tunnel stability is more significantly affected by reductions in cohesion and internal friction angle, while increases in these parameters and overburden depth have a less pronounced effect on displacement. These findings provide practical insights into the design and safe operation of unsupported sublevel stopes in carbonate-hosted lead–zinc deposits.

KEYWORDS

Sublevel stoping, underground mine stability, numerical modeling, rock mass sensitivity, FLAC2D, geomechanical properties, Lead–Zinc deposits

I. INTRODUCTION

Underground mining operations are inherently associated with complex geotechnical challenges, where the stability of excavations plays a critical role in ensuring worker safety, operational continuity, and economic viability (Rahimi et al., 2021; Chehreghani et al., 2022; Salmi et al., 2024; Nabavi et al., 2025). Ground control issues, including rockfalls, roof collapses, and progressive instability of underground openings, remain among the leading causes of accidents, ore dilution, equipment damage, production delays, and fatalities in hard-rock mining worldwide (Idris, 2014; Cordova et al., 2024; Army et al., 2026). Accurate assessment and prediction of excavation stability are therefore essential prerequisites for safe and cost-effective mining (Sharp, 2011; Khan et al., 2024; Kumar et al., 2025).

In recent decades, unsupported (self-supporting) mining methods have attracted increasing interest owing to their economic benefits, particularly in competent rock masses where artificial support systems can be minimized or eliminated (Alpay and Yavuz, 2009; Kaklis et al., 2021; Mijalkovski et al., 2021; Darling, 2023). Among these techniques, sublevel stoping (including variants such as long-hole and open stoping) is widely employed for steeply dipping orebodies in hard-rock environments because it enables high production rates while relying primarily on the inherent strength and structural integrity of the surrounding rock mass (Pakalnis and Hughes, 2011; Dunwen, 2026).

[1] Department of Mining Engineering, Faculty of Engineering, University of Kashan, Kashan, Iran
M. Noorian-Bidgoli: noriyan@kashanu.ac.ir

Sublevel stoping is particularly sensitive to design and geomechanical conditions, as the absence of systematic artificial support makes excavation stability highly dependent on rock mass quality, in-situ stress conditions, and stope geometry (Dzimunya, 2018; Sari and Kumral, 2020; Khakimov and Urinov, 2021; Morales et al., 2022). Previous studies have highlighted the critical role of design parameters such as span, height, and blasting patterns in controlling overbreak and dilution during extraction (Germain and Hadjigeorgiou, 1997; Mawdesley et al., 2001). The stability of open stopes has been extensively investigated using empirical and analytical approaches, particularly the stability graph method and its subsequent modifications, which provide practical guidelines for stope design under varying geomechanical conditions (Suorineni et al., 2001). Furthermore, geotechnical characterization and numerical modeling have been recognized as essential tools for improving the reliability of stability assessments in sublevel stoping mines (Chen et al., 1983; Villaescusa, 2014).

Over the past few decades, significant efforts have been made to enhance sublevel stoping performance through optimization techniques, including production scheduling, stope boundary design, and dilution control using mathematical programming approaches (Grieco and Dimitrakopoulos, 2007; Copland and Nehring, 2016; Sotoudeh et al., 2020). Moreover, advanced computational approaches, such as machine learning and integrated digital platforms, have improved the prediction of dilution and stability performance in complex mining environments (Vallejos et al., 2015; Jorquera et al., 2023).

A wide range of methods has been developed to evaluate the stability of underground excavations, encompassing empirical approaches (e.g., Mathews–Potvin stability graph), analytical solutions, and advanced numerical modeling (Potvin et al., 1988; Heidarzadeh et al., 2020; Lima et al., 2024). Numerical techniques, particularly finite-difference and finite-element methods, have proven highly effective in simulating complex stress distributions, heterogeneous rock mass behavior, and excavation-induced deformation under realistic in-situ conditions (Zhou et al., 2023; Cui et al., 2024; Santos et al., 2024). Software packages such as FLAC2D and FLAC3D are widely used in mining geomechanics for predicting displacement fields, stress concentrations, plastic yielding, and potential failure zones around underground openings (Cordova et al., 2024; Machuca et al., 2024; Thakur and Jain, 2024; Eneyew et al., 2026).

Numerous investigations have examined the influence of key geomechanical parameters—including stope geometry, overburden depth, in-situ stress regime, and rock mass properties—on excavation stability (Martin et al., 2003; Noorian-Bidgoli and Jing, 2014; Saeidi et al., 2021). Sensitivity and probabilistic analyses have been widely applied to identify dominant factors and optimize mine design (Idris et al., 2011; Heidarzadeh, 2018). In addition, strain-based criteria such as the Sakurai critical strain criterion provide a practical framework for stability assessment, particularly when stress-based methods are difficult to apply (Sakurai, 1981; Sakurai et al., 1993; Daraei and Zare, 2019; Yiouta-Mitra and Sakurai, 2023).

Iran hosts substantial lead–zinc resources, many of which are carbonate-hosted deposits extracted using unsupported stoping methods in varied geological settings (Karimpour et al., 2017; Maghfouri et al., 2018; Esmaeili Sevieri et al., 2019; Rajabi et al., 2020). The Tajkuh lead–zinc mine, located in central Iran, represents a typical case where underground extraction is conducted at multiple levels with varying stope dimensions in relatively competent but heterogeneous rock masses (Ghorbani, 2012).

Despite the extensive application of numerical modeling for underground excavation stability assessment, limited studies have simultaneously integrated laboratory-derived geomechanical properties, numerical simulation, strain-based stability criteria, and sensitivity analysis for unsupported stopes in carbonate-hosted Pb-Zn deposits. Moreover, site-specific geomechanical investigations on Iranian underground lead–zinc mines employing sublevel stoping remain scarce. Therefore, the present study aims not only to evaluate the stability of underground openings in the Tajkuh mine through FLAC2D simulations, but also to quantify the relative influence of key geomechanical parameters—including tunnel dimensions, overburden depth, cohesion, and internal friction angle—on excavation stability. By combining laboratory testing, numerical modeling, Sakurai-based stability evaluation, and sensitivity analysis, this study provides practical insight into the geomechanical behavior of unsupported underground openings. It contributes to improving stability assessment strategies in similar carbonate-hosted mining environments.

II. MATERIALS AND METHODS

The evaluation of underground excavation stability in the Tajkuh lead–zinc mine required a comprehensive integration of site-specific geological, geomechanical, and mining data with advanced numerical modeling techniques. This section outlines the materials, laboratory testing procedures, and numerical methods employed to simulate the behavior of underground openings under varying tunnel geometries and overburden depths. Initially, representative rock samples were collected from active and previously mined areas of the deposit to determine key geomechanical properties, including density, elastic modulus, Poisson's ratio, cohesion, and internal friction angle. These parameters formed the basis for constructing a finite-difference numerical model using FLAC2D, which allowed investigation of roof displacement, stress redistribution, and overall stability for multiple tunnel cross-sections and depths.

This section describes the geological and structural characteristics of the Tajkuh deposit, the laboratory procedures used to determine mechanical properties of the rock, the tunnel geometries and mining configurations considered in the analysis, and the setup, boundary conditions, and implementation of numerical simulations. Together, these methods provide a robust framework to evaluate the stability of unsupported underground openings and to perform sensitivity analyses for critical geomechanical parameters.

A. Site description

The Tajkuh lead–zinc underground mine is located approximately 90 km from Bafq in Yazd Province. The mine is operated by Arya Falat Company, a subsidiary of Arya Fattah Middle East Holding. Geographically, the mine is situated in the Sabzdasht region in the southeastern part of Bafq. The nearest settlements to the mine are Basab and Tashkuiyeh villages. The distance from the mine to the city of Yazd is approximately 200 km. Access to the mine is provided via an asphalt road up to Tashkuiyeh village, followed by an unpaved road section of about 1.5 km. Fig. 1 shows an aerial view of the Tajkuh mine and its location within Yazd Province.

The study area is located in a semi-mountainous region characterized by a hot and arid climate. The maximum recorded temperature exceeds 45°C during summer, while minimum temperatures in winter can fall below freezing. The average annual precipitation is approximately 250 mm, mostly occurring from late autumn to early spring. The dominant wind direction is generally west–east, with secondary trends from north–south and northeast–southwest. Geographic coordinates for the corners of the mining area are (points of A, B, C, D, E) presented in Table 1.

Table 1. Geographic coordinates of the Tajkuh mine area

Point	Latitude (° ′ ″)	Longitude (° ′ ″)	UTM X (m)	UTM Y (m)
A	55°56′27″	31°27′24″	399368	3480699
B	55°58′21″	31°27′34″	402380	3480979
C	55°58′21″	31°26′19″	402358	3478669
D	55°57′17″	31°24′55″	400644	3476099
E	55°56′27″	31°24′55″	399324	3476112

The Tajkuh Pb–Zn deposit is located in the northeastern part of the 1:100,000 geological map of Basab within the Tabas–Posht-e-Badam metallogenic belt in central Iran. The geological setting is characterized predominantly by carbonate formations, where mineralization is structurally controlled and associated with relatively competent host rocks suitable for underground mining operations. The oldest rock units in the area belong to the Dahou series, deposited in a shallow marine environment, followed by the Kuhbanan Formation formed under higher-energy shallow marine conditions. Fig. 2 presents the geological map of the Tajkuh mine area, illustrating major formations and structural trends relevant to underground excavation behavior and geomechanical assessment.

Mining activities in the Tajkuh area date back to ancient times, as evidenced by old surface workings and vertical channels observed in the northern part of the deposit. Modern underground mining operations began in the mid-20th century.

Mineralization in the study area is primarily concentrated along structurally controlled zones with a general north–south trend. Lead–zinc mineralization occurs mainly in dolomitic host rocks of the Shotori Formation in the form of vein–veinlet systems, replacement structures, and open-space fillings.

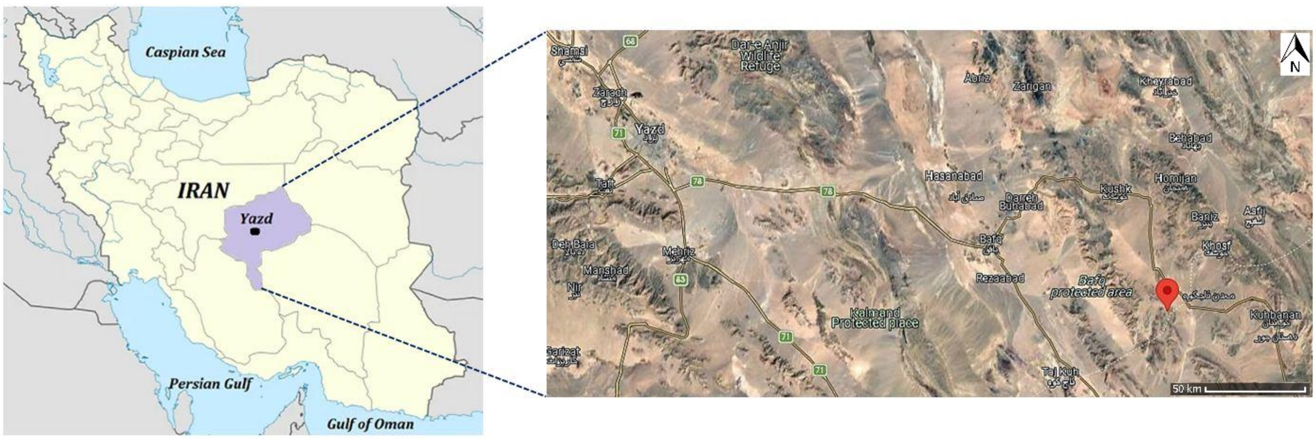

Fig. 1. Aerial view and location of the Tajkuh lead–zinc mine, Yazd Province, Iran

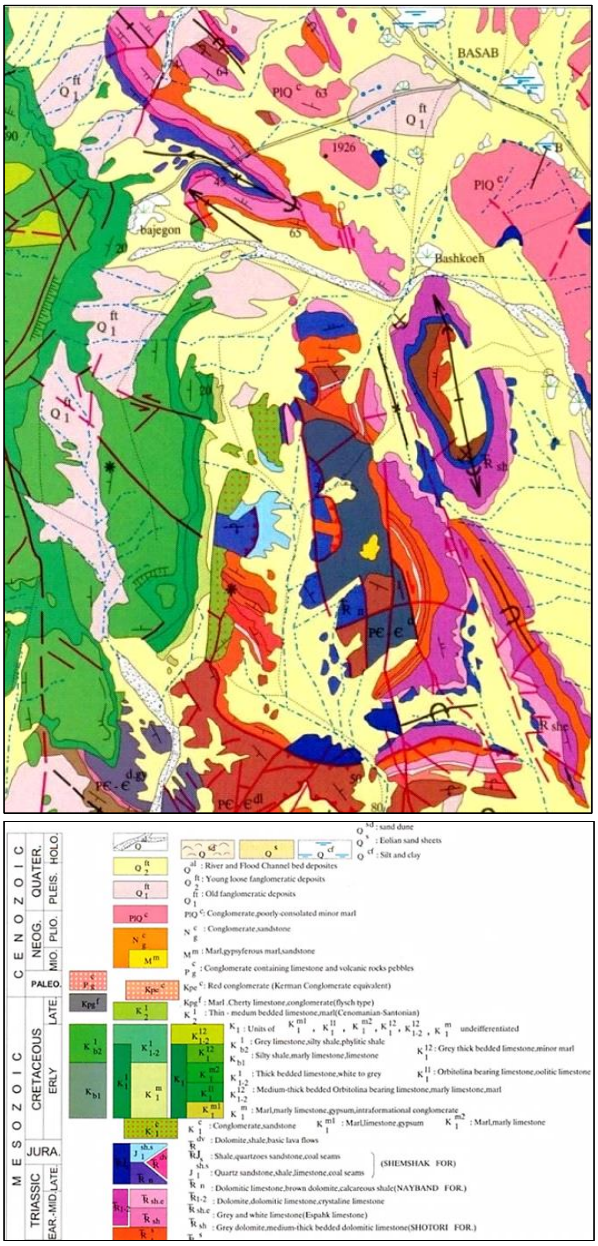

Fig. 2. Geological map of the Tajkuh lead–zinc mine area, showing major formations and structural trends

Two main types of ore are identified: sulfide and oxide. The sulfide ore, formed through hypogene hydrothermal processes, consists mainly of pyrite, sphalerite, galena, and marcasite. Mineralogical studies indicate that pyrite is the dominant sulfide mineral, often exhibiting euhedral cubic forms, while sphalerite is generally more abundant than galena.

The oxide ore, which represents the dominant ore type in surface exposures, is formed by weathering and oxidation of the primary sulfide mineralization. This ore is characterized by the presence of iron oxides and hydroxides, giving it a reddish to brownish color. Secondary minerals such as cerussite, anglesite, smithsonite, hemimorphite, and willemite are commonly observed.

From a structural perspective, the region is strongly influenced by the Kuhbanan Fault, which trends northwest–southeast and exhibits compressional movement with a right-lateral strike-slip component. This fault has played a major role in shaping the regional tectonic framework and has generated numerous subsidiary faults with varying orientations.

The Tajkuh deposit is located near the northern plunge of the Tajkuh anticline, which has an overall trend of N15W to N20W and a length of approximately 5 km. The steeply dipping limbs of the anticline, including locally overturned eastern limbs, indicate dominant compressive stresses from the west and southwest.

Mineralization is structurally controlled and occurs mainly in extensional zones associated with folding and faulting. The main mineralized zone extends over approximately 140 m with a thickness ranging from 2 to 15 m and a dip of about 80° toward the west. Additional smaller mineralized zones with lengths of 15–20 m and thicknesses of 1–3 m are also observed in the central part of the study area.

Based on geological, mineralogical, and structural characteristics, the Tajkuh lead–zinc deposit can be classified as a Mississippi Valley-Type (MVT) deposit. Evidence supporting this classification includes dolomitic host rocks, hydrothermal alteration, sulfide mineral assemblages, structural control, and the dominance of zinc over lead.

Underground mining at the Tajkuh lead–zinc mine is conducted using the sublevel stoping method, which is widely applied in steeply dipping ore bodies due to its high productivity and reliance on the inherent strength of the rock mass. In this method, extraction is carried out through a series of horizontal production drifts developed at different sublevels. A general view of the underground workings is shown in Fig. 3, illustrating the geometry and spatial distribution of the underground mining stope within the orebody.

According to reserve estimation based on geostatistical analysis, the total ore reserve of the main mineralized vein above a cutoff grade of 2% Zn is approximately 125,752 tonnes, with average grades of 3.44% Zn and 2.06% Pb. In addition, the proven extractable reserve is estimated at approximately 182,000 tonnes, with average grades of 8.1% Zn and 2.7% Pb, corresponding to an estimated metal content of about 14,742 tonnes of zinc and 4,914 tonnes of lead. Current mining operations have a production capacity of approximately 3,000 tonnes per month, equivalent to nearly 36,000 tonnes annually. Ore extraction is conducted through sublevel stoping using drilling and blasting sequences adapted to stope geometry and ore body continuity. Variations in extraction depth and excavation dimensions, combined with unsupported mining conditions, make stability assessment a critical requirement for safe and sustainable production at the mine.

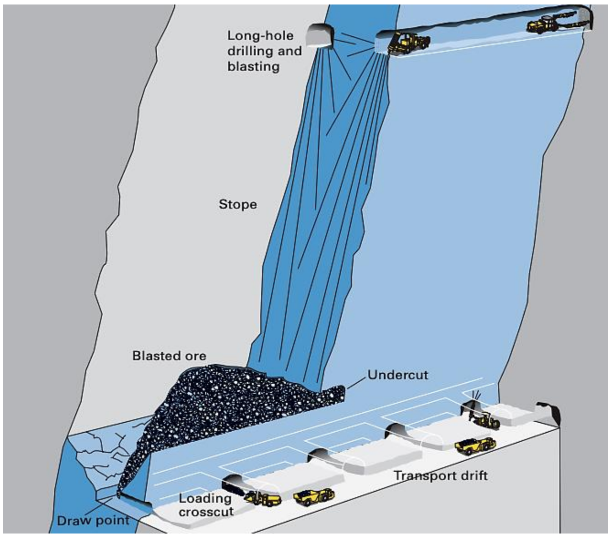

(a)

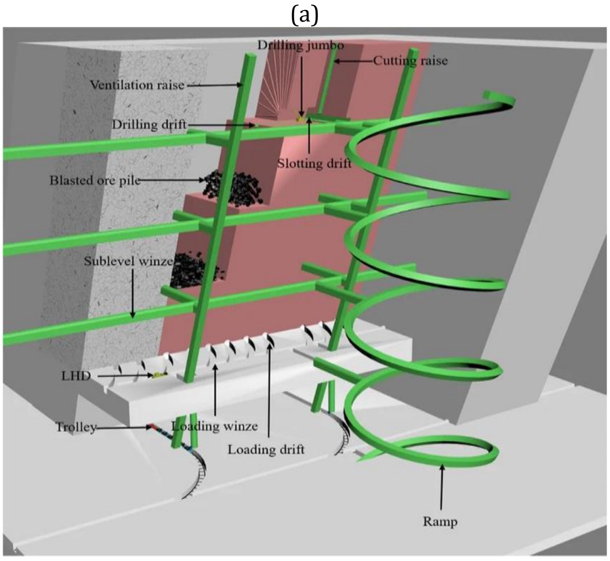

(b)

Fig. 3. Schematic illustration of the sublevel stoping mining method: (a) general layout of underground stopes and sublevels; (b) typical underground mine development openings, including drifts, raises, winzes, ramp, and sublevels used for access, ventilation, and ore extraction (Atlas Copco, 2022)

The orebody is accessed via a vertical shaft equipped with a skip hoisting system, which serves as the main haulage infrastructure for transporting ore to the surface. A longitudinal section of the deposit, including the shaft and ore zones, is presented in Fig. 4.

The production drifts typically have square cross-sections, with one of the common geometries being 2.5 × 2.5 m, as illustrated in Fig. 5. These openings are developed at multiple levels (e.g., 50, 60, 80, and 120 m), depending on the ore geometry and mining sequence.

In addition to the shaft system, auxiliary access between levels is provided by raises and inclined openings (winzes), facilitating ventilation, personnel movement, and ore transfer. The main shaft equipment used for hoisting operations is shown in Fig. 6.

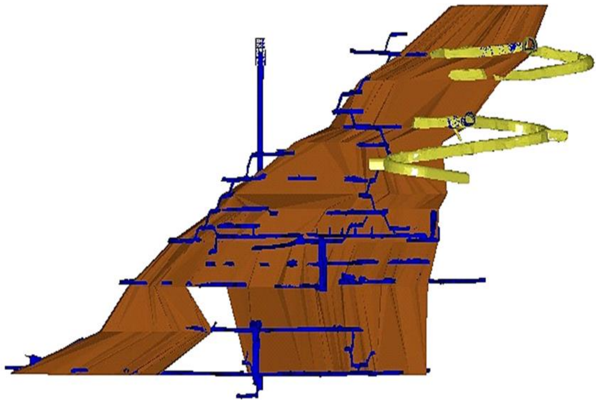

Fig. 4. Vertical section of the Tajkuh deposit showing the orebody and shaft system

Fig. 5. Typical cross-section (2.5 × 2.5 m) of extraction tunnels in the Tajkuh mine

The combination of vertical shaft access, horizontal sublevel development, and unsupported stopes makes this mining method highly dependent on the geomechanical behavior of the surrounding rock mass. Therefore, accurate stability assessment of these underground openings is essential for safe and efficient mining operations.

Underground mining at the Tajkuh mine is carried out using the sublevel stoping method, which is widely applied in lead–zinc deposits in Iran. Extraction is conducted through horizontal production drifts at multiple levels, typically at depths of 50, 60, 80, and 120 meters. The main access to the mine is provided by a vertical shaft equipped with a skip hoisting system for material transport.

Fig. 6. Main shaft hoisting system and equipment in the Tajkuh mine

Fig. 7. Intact cylindrical core samples collected from the Tajkuh lead–zinc mine

Fig. 8. Cylindrical rock specimens prepared for mechanical testing together with the compression testing system employed in the Rock Mechanics Laboratory

In addition, inclined raises and crosscuts with varying cross-sectional dimensions are used to connect different mining levels and provide access to the ore body. The unsupported nature of the stopes makes stability analysis a critical aspect of mine design and operation.

B. Geomechanical properties of rock

Accurate determination of geomechanical properties of the rock mass is a fundamental requirement for reliable numerical modeling in underground excavations. In this study, laboratory investigations were conducted to obtain the mechanical parameters of the host rock in the Tajkuh lead–zinc mine.

Rock samples were collected in the form of intact cylindrical core specimens obtained from previous exploratory drilling operations (Fig. 7). These samples were carefully selected to ensure minimal discontinuities. They were transported to the Rock Mechanics Laboratory of Yazd University for testing. Standard rock mechanics laboratory tests were performed in accordance with recommended procedures to determine the mechanical properties of the rock material.

Fig. 8 shows representative prepared specimens together with the compression testing apparatus used for determining the mechanical properties of the rock material. The laboratory program was designed to characterize the intact rock behavior under compressive loading conditions and to provide experimentally derived strength parameters to be used as input data for the FLAC2D simulations.

Laboratory testing was conducted to determine key geomechanical properties required for numerical modeling, including uniaxial compressive strength (UCS) tests to evaluate axial load-bearing capacity, triaxial compressive tests under varying confining pressures to estimate cohesion and internal friction angle, and density measurements to determine volumetric weight. Both dry and water-saturated samples were tested to consider potential moisture effects on mechanical behavior.

The resulting failure patterns of the specimens were carefully recorded, providing visual confirmation of the laboratory procedures and validating the quality of the core samples. Representative failure patterns obtained from laboratory compression tests on intact rock specimens collected from the Tajkuh mine are illustrated in Fig. 9. The tested samples predominantly exhibit axial splitting and shear-induced fracture surfaces, indicating brittle failure behavior under increasing compressive loading. The observed fracture mechanisms are generally consistent with the relatively high internal friction angle and competent nature of the carbonate host rocks. These results provide experimental evidence for the mechanical behavior of the intact rock and support the selection of the Mohr–Coulomb constitutive model adopted in the numerical simulations.

Fig. 9. Representative failure patterns of intact rock specimens after laboratory compression testing

The stress–strain responses obtained from laboratory compression tests are shown in Fig. 10. The curves indicate predominantly elastic behavior followed by abrupt post-peak strength reduction, reflecting brittle failure characteristics of the tested rock specimens. The limited plastic deformation prior to failure suggests relatively competent host rock conditions, which are compatible with unsupported underground extraction methods employed in the mine.

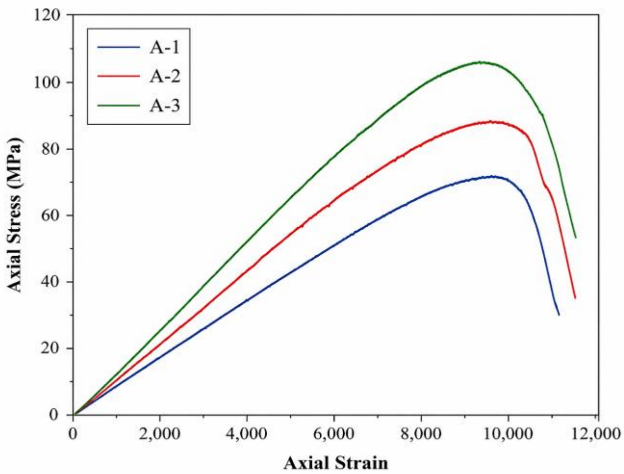

Fig. 10. Representative stress-strain curves obtained from laboratory compression tests on intact rock samples

Fig. 11 presents the Mohr–Coulomb failure envelope derived from triaxial compression test results. The tangent failure line fitted to the Mohr circles yielded an estimated cohesion value of approximately 2.28 MPa and an internal friction angle of 54.2°, indicating relatively high shear strength of the intact rock material. The agreement between experimental strength parameters and the adopted constitutive model confirms the suitability of the Mohr–Coulomb criterion for representing the mechanical behavior of the rock mass in subsequent numerical analyses.

The tests provided essential parameters, including uniaxial compressive strength, cohesion, internal friction angle, Poisson's ratio, and density, which were subsequently used as input for the FLAC2D numerical models. In this research, the Mohr–Coulomb failure criterion was adopted to describe the strength and deformation behavior of the rock mass. Accordingly, the required input parameters for numerical modeling include both strength and deformability characteristics. The obtained geomechanical parameters from laboratory tests are summarized as follows: density, elastic modulus, Poisson's ratio, cohesion, internal friction angle, and dilation angle. The average values of the determined parameters are presented in Table 2.

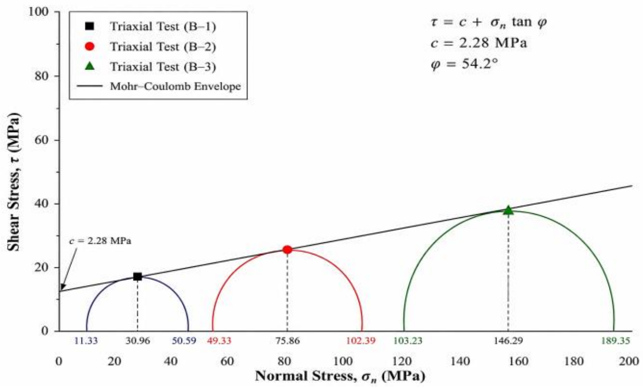

Fig. 11. Mohr–Coulomb failure envelope derived from triaxial compression tests showing estimated cohesion and internal friction angle of the intact rock

Table 2. Laboratory-derived geomechanical properties of the rock samples

Parameter	Unit	Value
Density	Kg/m^3	1889.2
Elastic Modulus	GPa	5.59
Poisson's Ratio	–	0.084
Cohesion	MPa	2.28
Friction Angle	degree	54.2

Based on these parameters, the bulk modulus and shear modulus required for numerical modeling were internally calculated by the FLAC2D software. These parameters were subsequently used as input data for simulating the mechanical behavior of underground excavations under different geometrical and stress conditions.

C. *Numerical modeling*

In this study, numerical simulations were carried out using the FLAC2D program, which is based on the finite difference method. This method is widely applied in geotechnical and mining engineering due to its capability to simulate complex stress–strain behavior and progressive failure in geomaterials.

The analysis focused on evaluating the stability of underground excavation openings with square cross-sections of 2.5×2.5 m^2, 3.5×3.5 m^2, and 4.5×4.5 m^2, located at depths of 30 m, 55 m, and 80 m below the ground surface. The rock mass behavior was simulated using the Mohr–Coulomb failure criterion, and the geomechanical parameters obtained from laboratory tests were assigned to the model.

In the present study, the rock mass was assumed to be homogeneous, isotropic, and continuous because detailed discontinuity mapping data were unavailable.

At the same time, field observations indicated relatively competent host rock conditions with insufficient information for explicit joint modeling. Therefore, the influence of discontinuities was not directly incorporated into the numerical simulations, and the surrounding rock was represented as an equivalent continuum medium. Based on these assumptions, the Mohr–Coulomb constitutive model was employed to describe rock mass behavior in the numerical analyses, as the required geomechanical parameters—including cohesion, internal friction angle, elastic modulus, and Poisson's ratio—were obtained directly from laboratory tests conducted on intact rock specimens collected from the Tajkuh mine. Furthermore, the Mohr–Coulomb failure criterion has been extensively applied in underground mining and excavation studies because it provides a practical representation of rock strength behavior using a limited number of parameters while maintaining acceptable predictive capability for preliminary stability assessments. Considering the objectives of this study and the absence of detailed discontinuity characterization, this constitutive model was considered appropriate for evaluating the stability of unsupported underground openings. The adopted assumptions represent a simplified but widely accepted approach for preliminary geomechanical assessment where detailed structural characterization data are limited.

The model dimensions were determined based on standard numerical modeling guidelines to minimize boundary effects. The lateral boundaries were located at a distance of approximately 10 times the tunnel width from the excavation, while the distance between the tunnel floor and model base was considered at least four times the tunnel height.

Accordingly, the model dimensions were defined as 55 m in width and 45 m in height. A uniform mesh was generated with a grid size of 0.5 m to ensure adequate resolution around the tunnel. To improve the accuracy and visualization of results, the final model consisted of a refined grid system of 120×120 elements.

The excavation geometry was created using a combination of linear and arc elements to represent the tunnel boundaries. This approach allowed a more realistic representation of the tunnel profile and reduced artificial stress concentrations in the roof region.

Appropriate boundary conditions were applied to ensure realistic simulation of in-situ conditions. The bottom boundary of the model was fixed in both horizontal and vertical directions, while the lateral boundaries were constrained in the horizontal direction only, allowing vertical displacement. This setup enabled simulation of ground behavior under the influence of gravity and lateral loads.

The initial stress field was applied based on gravitational loading using the following relationship:

$$\sigma_v = \rho . g . h \qquad (1)$$

Where ρ is the rock density, g is gravitational acceleration, and h is the depth. The horizontal stress was calculated using a stress ratio coefficient ($K = \sigma_h/\sigma_v$) of 0.18. The value of k was assigned according to the available mine-specific geological and geomechanical data. The model was assumed to be homogeneous and isotropic; therefore, the horizontal stresses in both directions were considered equal.

In cases where the overburden exceeded the model height, additional vertical stress was applied to the model surface using distributed loading to account for the extra overburden.

Before excavation, the model was brought to an initial equilibrium state under gravitational loading. This was achieved by solving the model in elastic mode until the maximum unbalanced force reached a negligible value, indicating static equilibrium.

To eliminate any pre-existing displacement effects, the displacement and velocity fields were reset to zero prior to excavation. This ensured that subsequent deformations were solely due to the excavation process.

Excavation was simulated in a single stage by assigning a null material to the tunnel region, representing complete removal of material. This approach is suitable for modeling unsupported excavations where no support system is installed.

During the simulation, monitoring points (history points) were defined at critical locations, including the tunnel roof, floor, and sidewalls. Vertical displacement (Y-direction) at the tunnel roof was considered the primary parameter for stability evaluation. In addition, horizontal displacements at the sidewalls and stress variations in the model were also recorded.

After excavation, the model was solved again until a new equilibrium state was achieved. The induced stress redistribution around the excavation resulted in deformation and displacement of the surrounding rock mass.

The results of the numerical simulations were evaluated using displacement contours and maximum roof displacement values. The maximum vertical displacement at the tunnel roof was used as the main criterion for assessing stability.

The results for different tunnel dimensions and depths were compared to investigate the influence of geometrical and stress parameters on excavation behavior. It was observed that increasing tunnel size and overburden depth leads to higher displacement values, indicating reduced stability conditions.

Detailed contour plots of displacement distribution and quantitative results of maximum roof displacement for all modeled scenarios are presented in the following section.

D. Stability assessment using the Sakurai critical strain criterion

The Sakurai critical strain criterion is a practical strain-based approach for evaluating the stability of underground excavations without requiring complex stress analysis. It compares the maximum principal strain induced around the opening (obtained from field measurements or numerical simulations) with a critical strain threshold, defined as the ratio of the uniaxial compressive strength to the Young's modulus of the rock or rock mass. According to Sakurai, the critical strain for rocks typically ranges between 0.1% and 1.0%; if the computed maximum strain exceeds this threshold, it indicates potential instability, and appropriate support measures may be needed. This method is particularly useful as a complementary tool in numerical modeling (e.g., FLAC2D) because it directly utilizes displacement results and provides a simple yet effective hazard warning level for assessing unsupported stopes and tunnels (Sakurai, 1997).

In the present study, strains derived from FLAC2D simulations were compared with Sakurai's critical limits to assess the stability condition of underground openings under varying tunnel dimensions and overburden depths. The application of this criterion enables interpretation of displacement behavior in terms of geomechanical stability and potential support requirements.

III. RESULTS AND DISCUSSION

The results obtained from the numerical simulations provide a comprehensive basis for evaluating the stability of underground openings in the Tajkuh lead–zinc mine. In this section, the effects of key design parameters, including tunnel cross-section and overburden depth, on deformation behavior are systematically analyzed. The distribution of displacement around the excavation, particularly at the tunnel roof, is examined through both quantitative results and contour plots. Furthermore, the stability of the excavations is assessed using the Sakurai critical strain criterion to determine whether the induced deformations remain within allowable limits. Finally, a sensitivity analysis is conducted to evaluate the influence of variations in rock mass properties on tunnel performance. This integrated approach enables a thorough understanding of the governing mechanisms controlling excavation stability and provides practical insights for the design and operation of unsupported underground spaces.

A. Effect of tunnel geometry and overburden on roof displacement

The results of numerical simulations for different tunnel cross-sections and overburden depths are summarized in Table 3. As shown in this table, the maximum roof displacement increases systematically with both the enlargement of tunnel cross-section and the increase in overburden depth. The minimum displacement value (0.3 mm) corresponds to the smallest tunnel dimension (2.5 × 2.5 m) at a shallow depth of 30 m, whereas the maximum displacement (2.0 mm) is observed for the largest tunnel (4.5 × 4.5 m) at 80 m depth.

Table 3. Maximum roof displacement for different tunnel cross-sections and overburden depths

Tunnel cross-section (m × m)	Overburden (m)	Max roof displacement (mm)
2.5 × 2.5	30	0.3
2.5 × 2.5	55	0.6
2.5 × 2.5	80	0.8
3.5 × 3.5	30	0.5
3.5 × 3.5	55	0.75
3.5 × 3.5	80	1.25
4.5 × 4.5	30	0.75
4.5 × 4.5	55	1.25
4.5 × 4.5	80	2

This trend clearly indicates that tunnel geometry plays a dominant role in deformation behavior. Larger excavations result in higher stress redistribution and reduced confinement, leading to greater deformation. Simultaneously, increasing overburden depth leads to higher in-situ stresses, which further amplify displacement values. However, the increase in displacement with depth is gradual, suggesting that the rock mass exhibits relatively competent behavior under increasing stress conditions.

B. Displacement distribution around the excavation

The distribution of vertical displacement around the tunnel for different geometries and depths is illustrated in Fig.s 12 to 14. These figures present contour plots of displacement in the vertical direction (Y-axis), providing insight into deformation patterns.

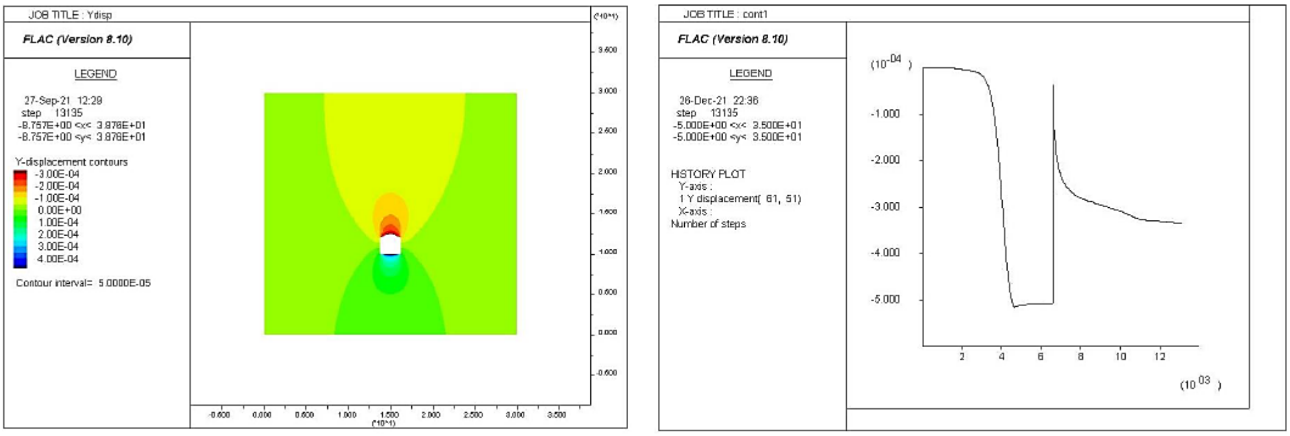

(a)

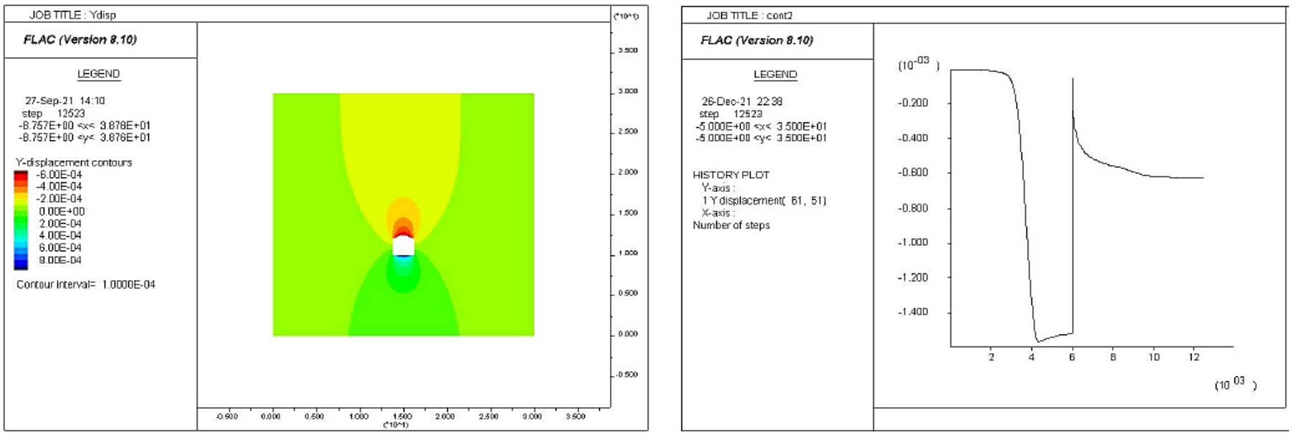

(b)

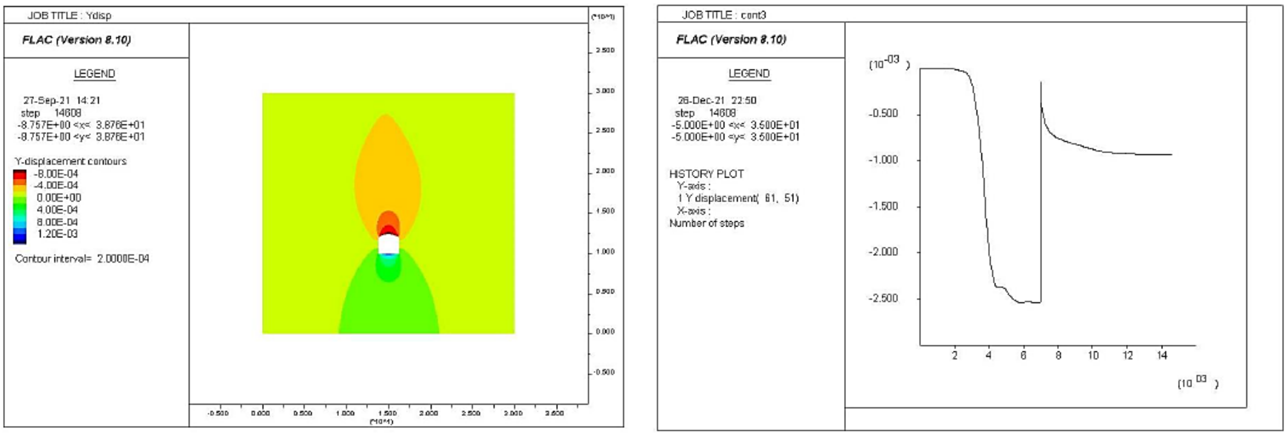

(c)

Fig. 12. Numerical results for the 2.5 × 2.5 m tunnel at three overburden depths: (a) 30 m, (b) 55 m, and (c) 80 m. Left panels: Contour plots of vertical displacement (Y-direction) showing overall deformation around the tunnel for each depth. Right panels: Maximum roof displacement highlighting deformation specifically at the tunnel roof for each depth

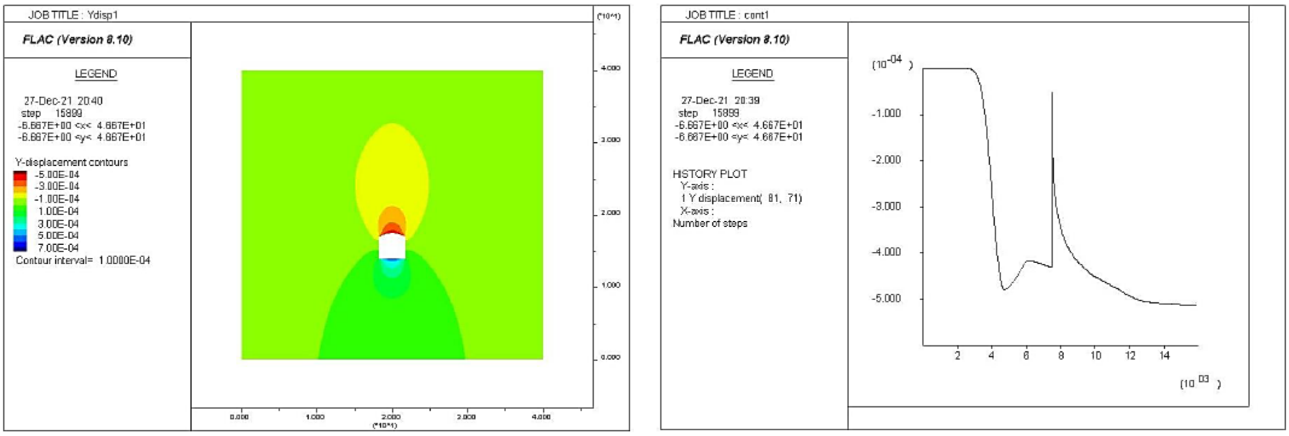

(a)

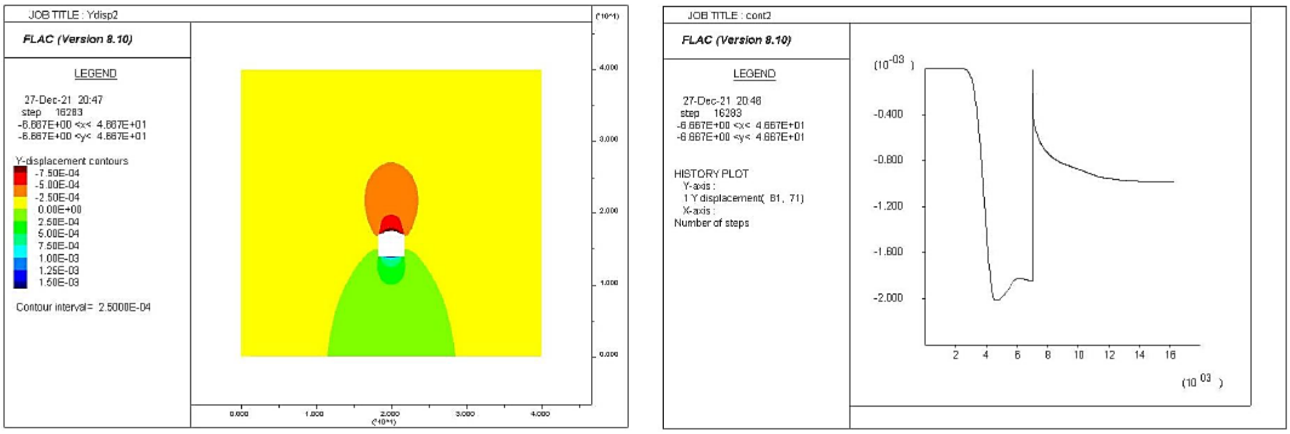

(b)

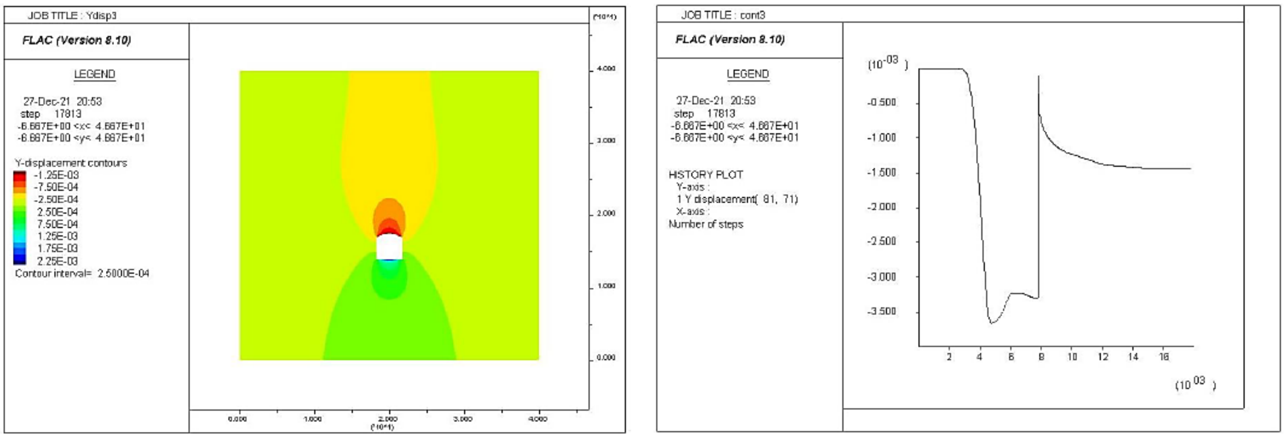

(c)

Fig. 13. Numerical results for the 3.5 × 3.5 m tunnel at three overburden depths: (a) 30 m, (b) 55 m, and (c) 80 m. Left panels: Contour plots of vertical displacement (Y-direction) showing overall deformation around the tunnel for each depth. Right panels: Maximum roof displacement highlighting deformation specifically at the tunnel roof for each depth

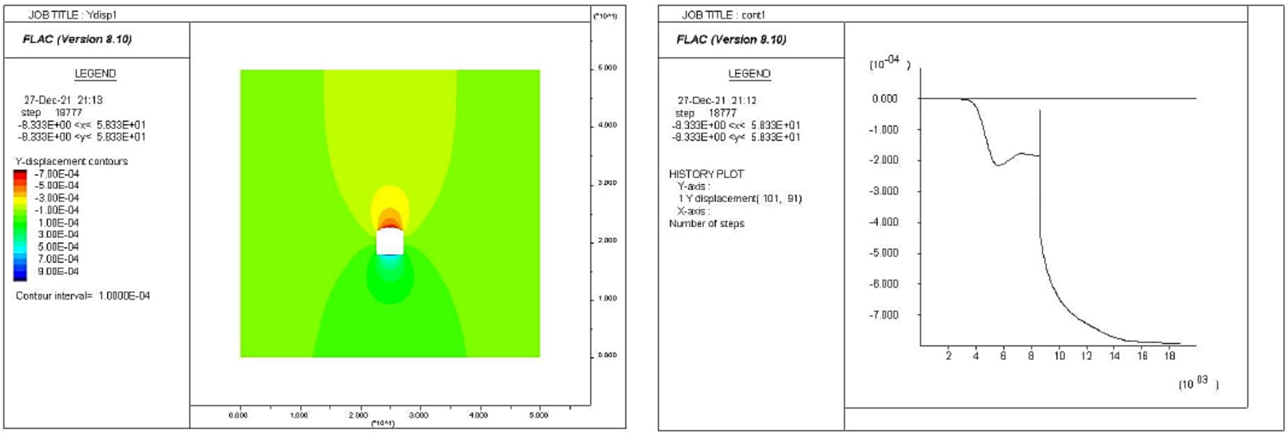

(a)

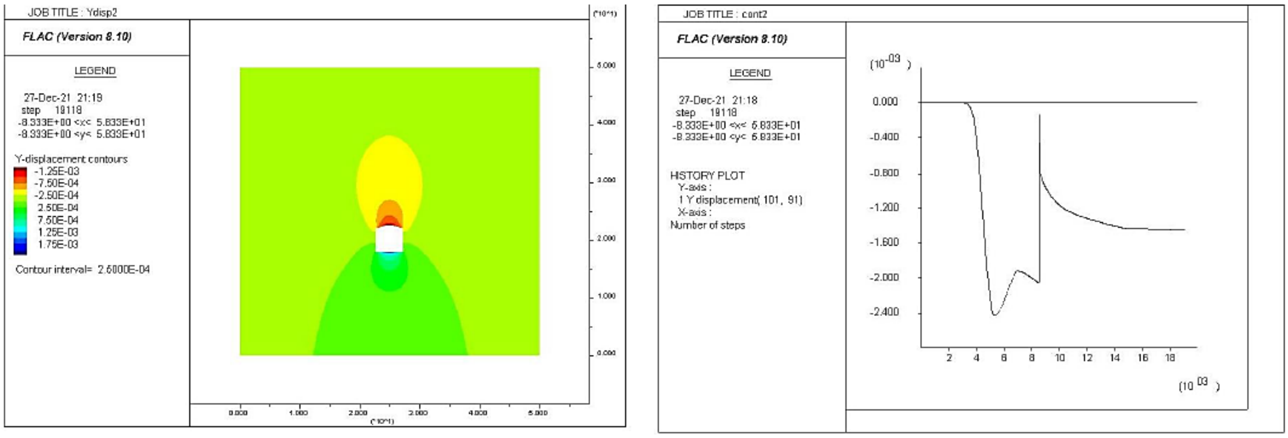

(b)

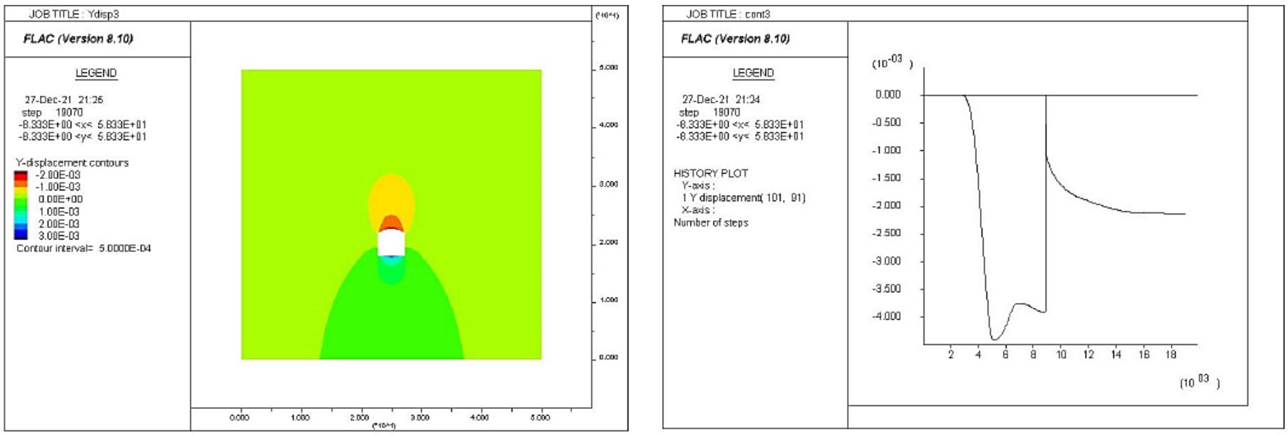

(c)

Fig. 14. Numerical results for the 4.5 × 4.5 m tunnel at three overburden depths: (a) 30 m, (b) 55 m, and (c) 80 m. Left panels: Contour plots of vertical displacement (Y-direction) showing overall deformation around the tunnel for each depth. Right panels: Maximum roof displacement highlighting deformation specifically at the tunnel roof for each depth

The contour plots reveal that deformation is primarily concentrated at the tunnel roof, with a gradual decrease toward the sidewalls and floor. This behavior is consistent with the redistribution of vertical stresses following excavation. As tunnel dimensions increase, the extent of the plastic zone around the excavation also expands, resulting in a wider deformation field.

Furthermore, increasing overburden depth leads to higher displacement magnitudes, although the pattern of deformation remains similar. The concentration of displacement at the roof suggests that this region is the most critical in terms of stability assessment, particularly in unsupported excavation conditions.

C. Stability evaluation based on Sakurai criterion

To evaluate the stability of the tunnels, the numerical results were compared with allowable displacement values obtained from the Sakurai critical strain criterion. The relationship between rock mass modulus and critical strain is shown in Fig. 15, which forms the basis for determining allowable deformation limits.

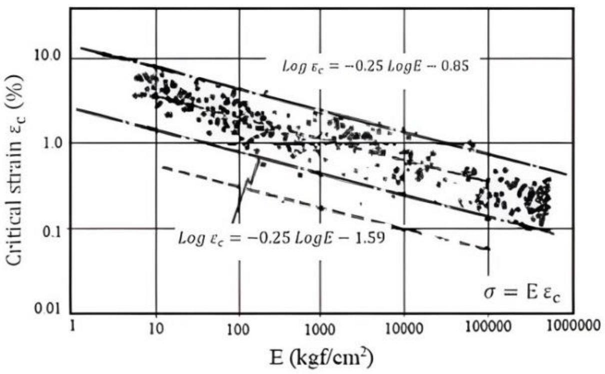

Fig. 15. Relationship between rock modulus and critical strain based on the Sakurai method

A comparison between the maximum roof displacement obtained from numerical modeling and the allowable displacement values is presented in Table 4.

Table 4. Comparison of numerical results with Sakurai allowable displacement values

Tunnel cross-section (m × m)	Overburden (m)	Max roof displacement (mm)	Sakurai allowable displacement (mm)
2.5 × 2.5	30	0.3	4.875
2.5 × 2.5	55	0.6	4.875
2.5 × 2.5	80	0.8	4.875
3.5 × 3.5	30	0.5	6.825
3.5 × 3.5	55	0.75	6.825
3.5 × 3.5	80	1.25	6.825
4.5 × 4.5	30	0.75	8.775
4.5 × 4.5	55	1.25	8.775
4.5 × 4.5	80	2	8.775

The results indicate that, in all cases, the computed displacements are significantly lower than the permissible limits defined by the Sakurai criterion. Even for the most critical condition (4.5 × 4.5 m tunnel at 80 m depth), the displacement remains well below the allowable threshold. This confirms that the excavations are stable and do not require additional support under the current geomechanical conditions.

These findings highlight the adequacy of the rock mass strength in maintaining stability, even in relatively large and deep underground openings.

D. Sensitivity analysis of geomechanical parameters

Prior to evaluating the influence of individual geomechanical parameters, it is essential to assess the overall stability behavior of the excavations under baseline conditions. The results presented in the previous sections indicate that tunnel geometry and overburden depth govern the general deformation pattern, with displacement primarily concentrated at the roof and increasing with excavation size and depth. However, these results alone do not fully capture the potential variability associated with uncertainties in rock mass properties. In practice, parameters such as cohesion and internal friction angle may vary due to geological heterogeneity, blasting effects, and structural discontinuities. Therefore, a sensitivity analysis is required to quantify the relative impact of these parameters on tunnel stability and to identify the controlling factors under different excavation dimensions. This approach provides a more comprehensive understanding of system behavior and enhances the reliability of the stability assessment for unsupported underground openings.

To further investigate the influence of rock mass properties on tunnel stability, a sensitivity analysis was conducted by varying the cohesion and internal friction angle of the rock mass by ±10%. The analysis was performed for all three tunnel cross-sections (2.5 × 2.5 m, 3.5 × 3.5 m, and 4.5 × 4.5 m) to evaluate the relative importance of these parameters under different geometric conditions.

The results indicate that increasing either cohesion or internal friction angle leads to only marginal reductions in roof displacement across all tunnel sizes. This suggests that the rock mass in its current state already provides sufficient strength, and further improvements in strength parameters do not significantly enhance stability.

In contrast, a reduction in these parameters results in a noticeable increase in displacement, particularly when both cohesion and friction angle are decreased simultaneously. This effect is more pronounced in smaller tunnel sections, where the stability is more directly controlled by material strength. For the 2.5 × 2.5 m tunnel, reductions in cohesion and friction angle lead to a relatively higher percentage increase in displacement compared to larger tunnels.

For medium-sized tunnels (3.5 × 3.5 m), the sensitivity remains evident but less pronounced, indicating a transition from material-controlled behavior toward geometry-influenced stability. In the largest tunnel section (4.5 × 4.5 m), although absolute displacement values are higher, the relative sensitivity to changes in geomechanical parameters decreases. This suggests that in larger excavations, geometric factors and stress redistribution play a more dominant role than minor variations in material strength.

Fig. 16 presents the results of the parametric sensitivity analysis conducted to evaluate the influence of rock strength parameters on underground excavation stability. The analysis demonstrates that progressive reductions in either cohesion or internal friction angle lead to gradual increases in normalized roof displacement. However, the simultaneous reduction of both parameters produces a substantially greater increase in deformation compared with individual parameter variations.

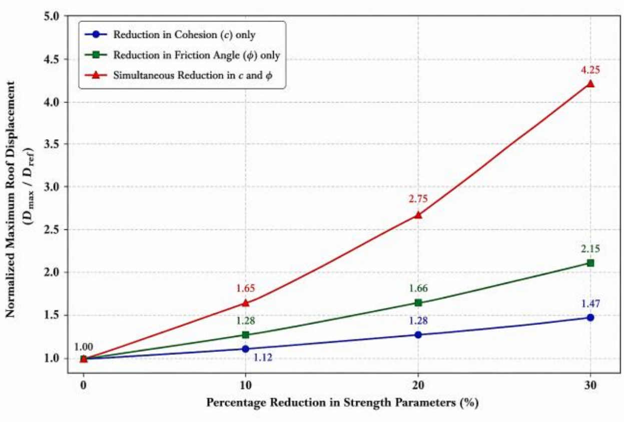

Fig. 16. Relationship between rock modulus and critical strain based on the Sakurai method

Among the investigated parameters, the combined decrease in cohesion and friction angle exhibits the strongest influence on excavation response, indicating the coupled role of shear strength properties in controlling tunnel stability. The results further suggest that isolated variations in cohesion produce relatively moderate displacement changes, whereas reductions in friction angle result in more pronounced deformation, particularly at larger parameter reductions.

Overall, the observed trends confirm that excavation stability in unsupported underground openings is highly sensitive to the degradation of rock shear strength properties. These findings highlight the importance of accurate geomechanical characterization and appropriate strength parameter selection in numerical modeling and underground mine design.

E. Overall stability assessment

Based on the combined analysis of displacement results, contour distributions, Sakurai criterion evaluation, and sensitivity analysis, it can be concluded that the underground openings in the Tajkuh mine are stable under the investigated conditions. Although displacement increases with tunnel size and depth, all values remain within acceptable limits.

The results also emphasize that while the current rock mass conditions are sufficient to maintain stability without support, any potential reduction in cohesion or internal friction angle—due to weathering, fracturing, or blasting damage—could significantly affect stability. Therefore, continuous monitoring and periodic reassessment of rock mass properties are recommended for long-term safety.

IV. CONCLUSION

In this study, the stability of underground excavations in the Tajkuh lead–zinc mine was investigated using numerical modeling based on the finite difference method. The effects of tunnel dimensions and overburden depth on the deformation behavior of underground openings were systematically analyzed. Based on the obtained results, the following conclusions can be drawn:

1. The results of numerical modeling indicate that both tunnel cross-sectional area and overburden depth have a direct impact on the magnitude of roof displacement. Increasing the tunnel dimensions from 2.5×2.5 m^2 to 4.5×4.5 m^2 significantly increases deformation.

2. The maximum roof displacement was observed in the largest tunnel section (4.5×4.5 m^2) at a depth of 80 m, with a value of approximately 2 mm. In contrast, the minimum displacement (0.3 mm) occurred in the smallest tunnel section (2.5×2.5 m^2) at a depth of 30 m

3. Comparison of the numerical results with the Sakurai criterion shows that the maximum displacements in all modeled scenarios are significantly lower than the allowable displacement limits. Therefore, the investigated underground openings are stable and do not require support systems under the studied conditions

4. The sensitivity analysis revealed that tunnel stability is more sensitive to reductions in cohesion and internal friction angle than to their increase. A decrease in these parameters leads to a noticeable increase in roof displacement, indicating the importance of maintaining rock mass strength properties.

5. Among the investigated parameters, cohesion plays a more dominant role in controlling tunnel stability compared to the internal friction angle.

Overall, the results of this study demonstrate that the rock mass conditions in the Tajkuh mine provide sufficient self-supporting capacity for the analyzed excavation geometries. However, potential degradation of rock mass properties due to geological or operational factors should be carefully considered in future mine design and stability assessments. The results of this study provide a reliable basis for the design and optimization of unsupported underground excavations. They can be effectively applied to similar lead–zinc deposits with comparable geological and geomechanical characteristics.

Beyond the site-specific findings obtained for the Tajkuh mine, this study demonstrates an integrated framework for stability assessment of unsupported underground openings by combining laboratory characterization, continuum-based numerical modeling, Sakurai strain criterion, and sensitivity analysis. The results indicate that, although tunnel geometry and overburden depth significantly influence displacement behavior, reductions in cohesion and internal friction angle exert greater control on excavation stability. These findings highlight the importance of accurately characterizing geomechanical properties during mine design and support the application of sensitivity-based approaches for identifying critical stability parameters in underground stoping operations. The proposed methodology may be extended to similar carbonate-hosted Pb–Zn deposits and unsupported mining systems where detailed structural information is limited. Accordingly, the present work moves beyond conventional displacement assessment and provides a more comprehensive basis for risk-informed geomechanical evaluation of unsupported stopes in deep underground mining.

REFERENCES

Alpay, S., & Yavuz, M. (2009). Underground mining method selection by decision making tools. Tunnelling and Underground Space Technology, 24(2), 173-184.

An, H., & Mu, X. (2025). Contributions to rock fracture induced by high ground stress in deep mining: a review. Rock Mechanics and Rock Engineering, 58(1), 463-511.

Army, M., Karian, T., Sasaoka, T., Hamanaka, A., Baskoro, F. R., Sulistianto, B., & Shimada, H. (2026). Optimization of Stope Dimensions in Geotechnically Complex Mine Using Automated Stability Analysis. Rudarsko-geološko-naftni zbornik, 41(2), in-Press.

Atlas copco (2022). Mining methods in underground mining. https: //miningandblasting.wordpress.com.

Chehreghani, S., Sola, H. A., & Chakeri, H. (2022). Stability analysis and support system design of Angouran underground mine batching room. Mining of Mineral Deposits, 16(1).

Chen, D. W., Chen, J. Y., & Zavokni, Z. M. (1983). Stability analysis of sublevel open stopes at great depth. In ARMA US Rock Mechanics/Geomechanics Symposium (pp. ARMA-83). ARMA.

Copland, T., & Nehring, M. (2016). Integrated optimization of stope boundary selection and scheduling for sublevel stoping operations. Journal of the Southern African Institute of Mining and Metallurgy, 116(12), 1135-1142.

Cordova, D. P., Gonçalves, Í. G., & Zingano, A. C. (2024). Optimizing stopes and rib pillars in sublevel open stoping mining method: an automated numerical modeling approach. COBRAMSEG, 6137-6144.

Cordova, D. P., Zingano, A. C., & Gonçalves, I. G. (2024). A heuristic methodology for economic and geomechanical optimization in sublevel open stoping mining method. Mining, Metallurgy & Exploration, 41(4), 1645-1657.

Cui, X., Yang, S., Zhang, N., & Zhang, J. (2024). Optimization of stope structure parameters by combining Mathews stability chart method with numerical analysis in Halazi iron mine. Heliyon, 10(4).

Daraei, A., & Zare, S. (2019). Modified criterion for prediction of tunnel deformation in non-squeezing ground conditions. Journal of Modern Transportation, 27(1), 11-24.

Darling, P. (Ed.). (2023). SME underground mining handbook. Society for Mining, Metallurgy & Exploration.

Dunwen, L. (2026). Sublevel Stoping Mining Method. In The ECPH Encyclopedia of Mining and Metallurgy (pp. 2079-2081). Singapore: Springer Nature Singapore.

Dzimunya, N. (2018). Design and dimensioning of sublevel stoping for extraction of thin ore (12 m) at very deep level: a case study of konkola copper mines (kcm), Zambia. Mathematical Modelling of Engineering Problems.

Eneyew, D. M., Adamu, A. Y., Ejigu, A. A., Nigussie, A. B., Endalew, S. A., Yalew, M. G., Kebede, B., Zeleke, S., Techane, G. and Assefa, D. (2026). Stability Assessment and Pillar Design of Underground Drift in Opal-Bearing Rock Masses: A Case Study from Wollo Opal Mining, Ethiopia. Geotechnical and Geological Engineering, 44(1), 19.

Esmaeili Sevieri, A., Karimpour, M. H., Malekzadeh Shafaroudi, A., Mahboubi, A., & Song, Y. (2019). Irankuh leadzinc mining district, southern Isfahan. Iran: Evidences of geology, fluid inclusion and isotope geochemistry, Periodico di Mineralogia, 88, 277-296.

Germain, P., & Hadjigeorgiou, J. (1997). Influence of stope geometry and blasting patterns on recorded overbreak. International Journal of Rock Mechanics and Mining Sciences, 34(3-4), 115-e1.

Ghorbani, M. (2012). Metallogenic and mining provinces, belts and zones of Iran. In The economic geology of Iran: Mineral deposits and natural resources (pp. 199-295). Dordrecht: Springer Netherlands.

Ghorbani, M., Shahriar, K., Sharifzadeh, M., & Masoudi, R. (2020). A critical review on the developments of rock support systems in high stress ground conditions. International Journal of Mining Science and Technology, 30(5), 555-572.

Grieco, N., & Dimitrakopoulos, R. (2007). Managing grade risk in stope design optimisation: probabilistic mathematical programming model and application in sublevel stoping. Mining technology, 116(2), 49-57.

Heidarzadeh, S. (2018). Probabilistic stability analysis of open stopes in sublevel stoping method by numerical modeling (Doctoral dissertation, Université du Québec à Chicoutimi).

Heidarzadeh, S., Saeidi, A., & Rouleau, A. (2020). Use of probabilistic numerical modeling to evaluate the effect of geomechanical parameter variability on the probability of open-stope failure: a case Study of the Niobec Mine, Quebec (Canada). Rock Mechanics and Rock Engineering, 53(3), 1411-1431.

Idris, M. A. (2014). Probabilistic stability analysis of underground mine excavations (Doctoral dissertation, Luleå tekniska universitet).

Idris, M. A., Saiang, D., & Nordlund, E. (2011). Probabilistic analysis of open stope stability using numerical modelling. International Journal of Mining and Mineral Engineering, 3(3), 194-219.

Jorquera, M., Korzeniowski, W., & Skrzypkowski, K. (2023). Prediction of dilution in sublevel stoping through machine learning algorithms. In IOP Conference Series: Earth and Environmental Science (Vol. 1189, No. 1, p. 012008). IOP Publishing.

Kaklis, K., Agioutantis, Z., Masialeti, M., Yendaw, J., & Betsi, T. B. (2021). Parametric analysis of Rib pillar stability in a longitudinal sublevel open stoping operation in an underground copper mine in southern Africa. Materials Proceedings, 5(1), 11.

Karimpour, M. H., Malekzadeh Shafaroudi, A., Esmaeili Sevieri, A., Saeed, S., Allaz, J. M., & Stern, C. R. (2017). Geology, mineralization, mineral chemistry, and ore-fluid conditions of Irankuh Pb-Zn mining district, south of Isfahan. Journal of Economic Geology, 9(2), 267-294.

Khakimov, S. I., & Urinov, S. R. (2021). Sublevel stoping with applying artificial hardening stowing pillars for extraction of veins in complicated geotechnical conditions. Mining Science and Technology (Russia), 6(4), 252-258.

Khan, M., Xueqiu, H., Jia, G., & Dazhao, S. (2024). Accurate prediction of indicators for engineering failures in complex mining environments. Engineering Failure Analysis, 155, 107736.

Kumar, M., Avchar, A., & Sinha, S. (2025). Integrated approaches for pillar design and stability assessment in underground hard rock mining: From empirical models to machine learning. Physics and Chemistry of the Earth, Parts A/B/C, 104235.

Lima, M. P. D., Guimarães, L. J. D. N., & Gomes, I. F. (2024). Numerical modeling of the underground mining stope stability considering time-dependent deformations via finite element method. REM-International Engineering Journal, 77, e230080.

Machuca, L., Lain, R., Silva, E., & Fleetwood, K. (2024). Case study of using Flac 3D numerical modelling in the prediction of stress-related deformation of a sill pillar in an underground metal mine and the response of a roadway inside the pillar during mining. In New challenges in rock mechanics and rock engineering (pp. 1538-1543). CRC Press.

Maghfouri, S., Hosseinzadeh, M. R., Rajabi, A., & Choulet, F. (2018). A review of major non-sulfide zinc deposits in Iran. Geoscience Frontiers, 9(1), 249-272.

Martin, C. D., Kaiser, P. K., & Christiansson, R. (2003). Stress, instability and design of underground excavations. International Journal of Rock Mechanics and Mining Sciences, 40(7-8), 1027-1047.

Mawdesley, C., Trueman, R., & Whiten, W. J. (2001). Extending the Mathews stability graph for open–stope design. Mining Technology, 110(1), 27-39.

Mijalkovski, S., Peltechki, D., Despodov, Z., Mirakovski, D., Adjiski, V., & Doneva, N. (2021). Methodology for underground mining method selection. Mining science, 28.

Morales, N., Mancilla, D., Miranda, R., & Vallejos, J. (2022). A fast method to develop an optimal operational sublevel stope design. Resources Policy, 77, 102670.

Nabavi, Z., Mirzehi, M., & Fayyazi, A. (2025). Underground Mine Planning, Scheduling, and Optimization: Current Trends and Challenges. Advancements in Underground Infrastructures, 125-146.

Noorian-Bidgoli, M., & Jing, L. (2014). Effects of loading conditions on strength and deformability of fractured rocks–a numerical study. In: Rock engineering and rock mechanics: Structures in and on rock masses, Proceedings of EUROCK. CRC Press. p. 365e8.

Pakalnis, R. T., & Hughes, P. B. (2011). Sublevel stoping. SME mining engineering handbook, 1, 1355-1363.

Potvin, Y., Hudyma, M., & Miller, H. D. S. (1988). The stability graph method for open stope design, 90th CIM AGM. Edmonton, May.

Rahimi, B., Sharifzadeh, M., & Feng, X. T. (2021). A comprehensive underground excavation design (CUED) methodology for geotechnical engineering design of deep underground mining and tunneling. International Journal of Rock Mechanics and Mining Sciences, 143, 104684.

Rajabi, A., Alfonso, P., Canet, C., Rastad, E., Niroomand, S., Modabberi, S., & Mahmoodi, P. (2020). The world-class Koushk Zn-Pb deposit, Central Iran: A genetic model for vent-proximal shale-hosted massive sulfide (SHMS) deposits–Based on paragenesis and stable isotope geochemistry. Ore geology reviews, 124, 103654.

Saeidi, A., Heidarzadeh, S., Lalancette, S., & Rouleau, A. (2021). The effects of in situ stress uncertainties on the assessment of open stope stability: case study at the Niobec Mine, Quebec (Canada). Geomechanics for Energy and the Environment, 25, 100194.

Sakurai, S. (1981). Direct strain evaluation technique in construction of underground opening. In ARMA US Rock Mechanics/Geomechanics Symposium (pp. ARMA-81). ARMA.

Sakurai, S. (1997). Lessons learned from field measurements in tunnelling. Tunnelling and underground space technology, 12(4), 453-460.

Sakurai, S., Kawashima, I., & Otani, T. (1993). A criterion for assessing the stability of tunnels. In ISRM EUROCK (pp. ISRM-EUROCK). ISRM.

Salmi, E. F., Phan, T., Sellers, E. J., & Stacey, T. R. (2024). A review on the geotechnical design and optimisation of ultra-long ore passes for deep mass mining. Environmental Earth Sciences, 83(10), 301.

Santos, A., Shnorhokian, S., & Kumral, M. (2024). Stability assessment for an extended stope in a case study underground mine. Itasca Symposium.

Sari, Y. A., & Kumral, M. (2020). A planning approach for polymetallic mines using a sublevel stoping technique with pillars and ultimate stope limits. Engineering Optimization, 52(6), 932-944.

Sharp, J. E. U. R. (2011). Applicability of the Mathews stability method to open stope stability assessment at Olympic Dam Mine (Doctoral dissertation, University of Canterbury).

Sotoudeh, F., Nehring, M., Kizil, M., Knights, P., & Mousavi, A. (2020). Production scheduling optimisation for sublevel stoping mines using mathematical programming: A review of literature and future directions. Resources Policy, 68, 101809.

Suorineni, F. T., Kaiser, P. K., & Tannant, D. D. (2001). Likelihood statistic for interpretation of the stability graph for open stope design. International Journal of Rock Mechanics and Mining Sciences, 38(5), 735-744.

Thakur, V., & Jain, S. C. (2024). Mapping & Analysis Of Roof Stress Distribution In An Underground Coal Mine Using FLAC 3D Software. Journal of Scientific Research and Technology, 45-52.

Vallejos, J. A., Miranda, O., Gary, C., & Delonca, A. (2015). Development of an integrated platform for stability analysis and design in sublevel stoping mines—MineRoc®. In Design Methods 2015: Proceedings of the International Seminar on Design Methods in Underground Mining (pp. 477-488). Australian Centre for Geomechanics.

Villaescusa, E. (2014). Geotechnical design for sublevel open stoping. CRC press.

Yiouta-Mitra, P., & Sakurai, S. (2023). Critical strain method incorporating calculation of equivalent HB strength parameters for back analysis during tunnel excavation. Tunnelling and Underground Space Technology, 140, 105252.

Zhou, K., Xu, H., Yang, C., Xiong, X., & Gao, F. (2023). Numerical simulation of underground mining-induced fault-influenced rock movement and its application. Sustainability, 15(6), 5197.